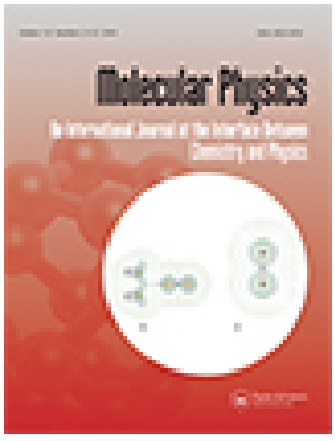

Molecular Physics: An International Journal at the Interface Between Chemistry and Physics

Publication details, including instructions for authors and subscription information:
http://www.tandfonline.com/loi/tmph20

An assessment of theoretical procedures for π-conjugation stabilisation energies in enones

Li-Juan Yu[a], Farzaneh Sarrami[a], Amir Karton[a] & Robert J. O'Reilly[b]

[a] School of Chemistry and Biochemistry, The University of Western Australia, Perth, Australia

[b] Department of Chemistry, School of Science and Technology, Nazarbayev University, Astana, Republic of Kazakhstan

Published online: 02 Dec 2014.

To cite this article: Li-Juan Yu, Farzaneh Sarrami, Amir Karton & Robert J. O'Reilly (2014): An assessment of theoretical procedures for π-conjugation stabilisation energies in enones, Molecular Physics: An International Journal at the Interface Between Chemistry and Physics, DOI: 10.1080/00268976.2014.986238

To link to this article: http://dx.doi.org/10.1080/00268976.2014.986238

Molecular Physics, 2014
http://dx.doi.org/10.1080/00268976.2014.986238

RESEARCH ARTICLE

An assessment of theoretical procedures for π-conjugation stabilisation energies in enones

Li-Juan Yu[a], Farzaneh Sarrami[a], Amir Karton[a,*] and Robert J. O'Reilly[b]

[a]*School of Chemistry and Biochemistry, The University of Western Australia, Perth, Australia;* [b]*Department of Chemistry, School of Science and Technology, Nazarbayev University, Astana, Republic of Kazakhstan*

(*Received 24 September 2014; accepted 5 November 2014*)

We introduce a representative database of 22 α,β- to β,γ-enecarbonyl isomerisation energies (to be known as the EIE22 data-set). Accurate reaction energies are obtained at the complete basis-set limit CCSD(T) level by means of the high-level W1-F12 thermochemical protocol. The isomerisation reactions involve a migration of one double bond that breaks the conjugated π-system. The considered enecarbonyls involve a range of common functional groups (e.g., Me, NH_2, OMe, F, and CN). Apart from π-conjugation effects, the chemical environments are largely conserved on the two sides of the reactions and therefore the EIE22 data-set allows us to assess the performance of a variety of density functional theory (DFT) procedures for the calculation of π-conjugation stabilisation energies in enecarbonyls. We find that, with few exceptions (M05-2X, M06-2X, BMK, and BH&HLYP), all the conventional DFT procedures attain root mean square deviations (RMSDs) between 5.0 and 11.7 kJ mol^{-1}. The range-separated and double-hybrid DFT procedures, on the other hand, show good performance with RMSDs below the 'chemical accuracy' threshold. We also examine the performance of composite and standard *ab initio* procedures. Of these, SCS-MP2 offers the best performance-to-computational cost ratio with an RMSD of 0.8 kJ mol^{-1}.

Keywords: enones; π-conjugation; isomerisation energies; density functional theory; CCSD(T)

1. Introduction

The relative thermodynamic stabilities of conjugated α,β- and the corresponding unconjugated β,γ-enecarbonyl derivatives (Scheme 1) are of general importance in organic and biochemistry. There has been strong interest in naturally occurring compounds that contain an α,β-enecarbonyl motif (Scheme 1). For example, a number of such compounds, including phenethyl caffeate [1] and ergolide [2] have been shown to exhibit strong inhibitory activity against the nuclear transcription factor NF-κB, [3] which plays a substantive role in inflammation and constitutive activity in malignant cells [4]. The β,γ-unsaturated structural motif, in which conjugation with the carbonyl moiety is lost, is also observed in a number of natural products, including molecules present in various fruits such as grapes (non-3-enoic acid) [5] and nectarines (methyl hex-3-enoate) [6].

The isomerisation between the α,β- and β,γ-forms of enecarbonyls also plays important roles in biochemical processes. For example, the enzyme β-hydroxydecanoyl thioester dehydrase catalyses the conversion of *trans*-α,β-decenoyl thioester to *cis*-β,γ-decenoyl thioester [7], a necessary step for introducing *cis* stereochemistry in fatty acids. Another example is the $\Delta^5 \rightarrow \Delta^4$-3-ketosteroid isomerase enzyme which catalyses the β,γ- to α,β-isomerisation of androst-5-ene-3,17-dione to androst-4-ene-3,17-dione [8,9]. From the perspective of synthetic organic chemistry, the isomerisation of β,γ-unsaturated ketones and their conjugated α,β-isomers (and vice versa) has been shown to be facilitated by both acids [10] and bases [11–13]. In addition to the use of acid or base catalysis, the synthesis of α,β-unsaturated (Z)-alkenes from β,γ-unsaturated ketones, by way of a Rh(I) catalyst, has also been documented recently [14].

A key contributing factor that governs the product that one may expect to obtain from a given reaction, be it the α,β- or β,γ-form, will be the energy separation between the two isomers. Regarding the relative stabilities of α,β- and β,γ-enecarbonyl compounds, experimental investigations have provided a number of findings, including for example: (1) the equilibrium between 5-methyl-4-hepten-3-one (α,β) and 5-methyl-5-hepten-3-one (β,γ) in acidic media was found to lie in favour of the former, with a ratio of 58:42 [15], and (2) β,γ-isomers are favoured at equilibrium in cases of the β-chloro and β-phenylthio-substituted ketones, but that hydrogen bonding between the carbonyl oxygen and the proton of a β-amino group stabilises the α,β-form [16]. Given the general importance of such isomerisation processes, it is desirable to consider more broadly the effect of substituents on the energetic separation across a wider range of enecarbonyl systems. This is not necessarily a trivial task using experimental methods, but can more readily be facilitated through accurate computational modelling.

* Corresponding author. Email: amir.karton@uwa.edu.au

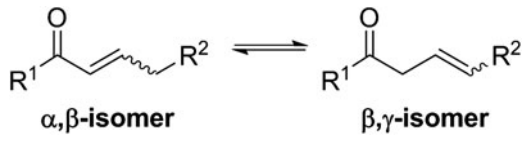

Scheme 1. Equilibrium between α,β- and β,γ-enecarbonyls.

We have recently carried out a systematic study on the performance of a variety of *ab initio* and density functional theory (DFT) procedures in predicting π-conjugation stabilisation energies in diolefins [17]. We found that many conventional DFT procedures have difficulty in describing reactions of the type: conjugated diolefin → non-conjugated diolefin, with root mean square deviations (RMSDs) from accurate isomerisation energies ranging between 4.5 and 11.7 kJ mol^{-1}. Double-hybrid DFT (DHDFT) and most *ab initio* procedures, on the other hand, show excellent performance with RMSDs well below the 'chemical accuracy' threshold (arbitrarily defined as 1 kcal mol^{-1} ≈ 4.2 kJ mol^{-1}). In this work, we proceed to investigate the broader ramifications of these findings for π-conjugation stabilisation energies in conjugated enecarbonyls in which the conjugated π-system is extended over C and heteroatoms (namely, O and N). Introducing an electronegative heteroatom into the π-system is expected to stabilise resonance structures with a negative charge on the heteroatom. We obtain highly accurate α,β- to β,γ-isomerisation energies using the W1-F12 thermochemical protocol for a diverse set of 22 enecarbonyl systems, which we refer to as the enecarbonyl isomerisation energies (EIE22) database [18]. The isomerisation reactions in the EIE22 database are of the type α,β-enecarbonyl → β,γ-enecarbonyl (Scheme 1). The considered enecarbonyls involve linear and cyclic structures with a spectrum of common functional groups, including Me, NH_2, OMe, F, and CN. The isomerisation reactions involve a migration of one double bond that breaks the conjugated π-system. We proceed to use our W1-F12 reference values to assess the performance of more approximate theoretical procedures for the isomerisation energies in the EIE22 database. We consider a variety of contemporary DFT and DHDFT procedures, as well as a number of composite and standard *ab initio* methods. We show that the difficulties that conventional DFT procedures have in describing π-conjugation stabilisation energies are not limited to conjugated diolefins but are extended to a variety of enecarbonyl species [17].

2. Computational methods

In order to obtain reliable reference isomerisation energies for the EIE22 database, calculations have been carried out using the high-level, *ab initio*, W1-F12 procedure [18] with the Molpro 2012.1 program suite [19]. W1-F12 theory (and its earlier version W1) [20,21] represents a layered extrapolation to the relativistic, all-electron CCSD(T)/CBS (coupled cluster with singles, doubles, and quasiperturbative triple excitations basis-set-limit energy). This composite theory includes scalar-relativistic, diagonal Born–Oppenheimer, zero-point vibrational energy (ZPVE), and enthalpic corrections and can achieve 'near-benchmark accuracy' for atomisation reactions [22,23]. For example, it is associated with a mean absolute deviation (MAD) of 2.1 kJ mol^{-1} for a set of 140 very accurate atomisation energies [18,20,21,24]. Nevertheless, it should be pointed out that for the isomerisation reactions in the EIE22 database, these theories should yield even better performance due to a large degree of systematic error cancelation between reactants and products [25–29]. Finally, we note that our W1-F12 isomerisation energies are expected to lie very close to the infinite basis-set-limit energies, as indicated by very small differences between W1-F12 and W2-F12 theories for a set of 48 isomerisation reactions involving diolefins. Namely, W1-F12 attains an RMSD of only 0.15 kJ mol^{-1} relative to the W2-F12 values (see also discussion in Ref. [17]).

W1-F12 theory combines explicitly correlated F12 techniques [30] with basis-set extrapolations in order to approximate the CCSD(T) basis-set-limit energy. Due to the drastically accelerated basis-set convergence of the F12 methods [31,32], W1-F12 is superior to the original W1 method in terms of computational cost [18]. For the sake of making the article self-contained, we will briefly outline the various steps in W1-F12 theory (for further details see Refs [18] and [33]). The Hartree–Fock component is extrapolated from the VDZ-F12 and VTZ-F12 basis sets, using the $E(L) = E_\infty + A/L^\alpha$ two-point extrapolation formula, with $\alpha = 5$ (where VnZ-F12 denotes the cc-pVnZ-F12 basis sets of Peterson *et al*. [31], which were specifically developed for explicitly correlated calculations). Note that the complementary auxiliary basis set singles correction is included in the self-consistent field (SCF) energy [34–36]. The valence CCSD-F12 correlation energy is extrapolated from the same basis sets, using the $E(L) = E_\alpha + A/L^\alpha$ two-point extrapolation formula, with $\alpha = 3.38$. Optimal values for the geminal Slater exponents (β) used in conjunction with the VnZ-F12 basis sets were taken from Ref. [32]. The (T) valence correlation energy is obtained from standard CCSD(T) [20], namely, extrapolated from the A′VDZ and A′VTZ basis sets using the above two-point extrapolation formula with $\alpha = 3.22$ (where A′VnZ indicates the combination of the standard correlation-consistent cc-pVnZ basis sets on H and the aug-cc-pVnZ basis sets on C, N, O, and F) [37,38]. In all of the explicitly correlated coupled cluster calculations the diagonal, fixed-amplitude 3C(FIX) ansatz [35,39–41], and the CCSD-F12b approximation are employed [36,42]. The CCSD inner-shell contribution is calculated with the core–valence weighted correlation-consistent cc-pwCVTZ basis set of Peterson and Dunning [43], whilst the (T) inner-shell contribution is calculated with the cc-pwCVTZ(no f) basis set (where

cc-pwCVTZ(no f) indicates the cc-pwCVTZ basis set without the f functions). The scalar relativistic contribution (in the second-order Douglas–Kroll–Hess approximation) [44,45] is obtained as the difference between non-relativistic CCSD(T)/A′VDZ and relativistic CCSD(T)/A′VDZ-DK calculations [46]. The diagonal Born–Oppenheimer corrections are calculated at the HF/cc-pVTZ level of theory using the CFOUR program suite [47].

Since W1-F12 represents a layered extrapolation to the all-electron CCSD(T) basis-set-limit energy, it is of interest to estimate whether the contributions from post-CCSD(T) excitations are likely to be significant. The percentage of the total atomisation energy accounted for by parenthetical connected triple excitations, $\%TAE_e[(T)]$, has been shown to be a reliable energy-based diagnostic for the importance of non-dynamical correlation effects. It has been suggested that $\%TAE_e[(T)] < 2\%$ indicates systems that are dominated by dynamical correlation, while $2\% < \%TAE_e[(T)] < 5\%$ indicates systems that include mild non-dynamical correlation [21,24,48]. Table S1 (Supplemental data) gathers the $\%TAE_e[(T)]$ values for the reactants and products involved in the EIE22 database. The $\%TAE_e[(T)]$ values for these species lie in the range 1.7%–2.4%. These values suggest that all the species in the EIE22 database are dominated by dynamical correlation effects, and that our bottom-of-the-well CCSD(T)/CBS benchmark isomerisation energies should be within 2–3 kJ mol^{-1} from the reaction energies at the full configuration interaction basis-set limit. We note that the cyano species (reactions 7 and 14–16, Figure 1) are characterised by the largest $\%TAE_e[(T)]$ values.

The geometries of all structures have been obtained at the B3LYP-D3/A′VTZ level of theory [49–52]. Empirical D3 dispersion corrections [53,54] are included using the Becke−Johnson [55] damping potential as recommended in Ref. [52] (denoted by the suffix -D3). Harmonic vibrational frequency analyses have been performed to confirm each stationary point as an equilibrium structure (i.e., all real frequencies). ZPVE and enthalpic corrections have been obtained from such calculations. All geometry optimisations and frequency calculations were performed using the Gaussian 09 program suite [56].

The DFT exchange-correlation functionals considered in this study (ordered by their rung on Jacob's Ladder) [57] are the pure generalised gradient approximation (GGA) functionals: BLYP [49,58], B97-D [59], HCTH407 [60], PBE [61], BP86 [58,62], BPW91 [58,63], SOGGA11 [64], N12 [65]; the meta-GGAs (MGGAs): M06-L [66], TPSS [67], τ-HCTH [68], VSXC [69], BB95 [70], M11-L [71], MN12-L [72]; the hybrid-GGAs (HGGAs): BH&HLYP [73], B3LYP [49–51], B3P86 [50,62], B3PW91 [50,63], PBE0 [74], B97-1 [75], B98 [76], X3LYP [77], SOGGA11-X [78]; the hybrid-meta-GGAs (HMGGAs): M05 [79], M05-2X [80], M06 [81], M06-2X [81], M06-HF [81], BMK [82], B1B95 [58,70], TPSSh [83], τ-HCTHh [68], PW6B95 [84], and the DHDFT procedures: B2-PLYP [85], B2GP-PLYP [86], B2K-PLYP [87], B2T-PLYP [87], DSD-BLYP [88], DSD-PBEP86 [89,90], PWPB95 [91]. We also consider the following range-separated (RS) functionals: CAM-B3LYP [92], LC-ωPBE [93], ωB97 [94], ωB97X [94], ωB97X-D [95], and M11 [96]. We note that the suffix -D in B97-D and ωB97X-D indicates the dispersion correction that was prescribed by the developers in Refs [59] and [95], rather than the D3 dispersion correction.

In addition, the performance of composite thermochemical procedures and standard *ab initio* methods is also assessed. We consider the following composite procedures: G4 [97], G4(MP2) [98], G4(MP2)-6X [99], G3 [100], G3(MP2) [101], G3B3 [102], G3(MP2)B3 [102], CBS-QB3 [103], and CBS-APNO [104], and the following *ab initio* methods: MP2, SCS-MP2 [105], MP2.5 [106], MP3, SCS-MP3 [107], MP4, CCSD, SCS-CCSD [108], SCS(MI)CCSD [109], and CCSD(T). The performance of the DFT and standard *ab initio* procedures is investigated in conjunction with the A′VnZ (n = D, T, and Q) correlation-consistent basis sets of Dunning and co-workers [37,38].

3. Results and discussion

3.1. Overview of the isomerisation reactions in the EIE22 database

The EIE22 database is comprised of 22 prototypical isomerisation reactions (shown in Figure 1) of the type:

$$\text{Conjugated enecarbonyl}(\alpha, \beta\text{-}) \rightarrow \text{Non-conjugated enecarbonyl}(\beta, \gamma\text{-}). \quad (1)$$

All the reactions involve a migration of one double bond, which breaks the conjugated π-system. Benchmark reference data have been obtained by means of the high-level W1-F12 procedure [18]. W1-F12 theory represents a layered extrapolation to the relativistic, all-electron CCSD(T) basis-set limit, and can achieve an accuracy in the kJ mol^{-1} range for molecules whose wave functions are dominated by dynamical correlation [18,20,21,24]. For the reactants involved in reactions **2** and **5**, experimental heats of formation at 298 K are available from the NIST thermochemical database [110]. Table S3 (Supplemental data) gives the W1-F12 heats of formation at 0 K ($\Delta H_{f,0}$) and 298 K ($\Delta H_{f,298}$) for the reactants and products involved in the EIE22 datbase. For the reactants of reactions **2** and **5**, we obtain $\Delta H_{f,298} = -150.0 \pm 3.8$ and -344.3 ± 3.8 kJ mol^{-1}, respectively [111]. The calculated heat of formation for the reactant in reaction **5** is in good agreement with the NIST experimental value (-342.3 ± 2.0 kJ mol^{-1}), in particular the computed and experimental values agree to within overlapping uncertainties. Our heat of formation for the reactant of reaction **2** is lower than the NIST

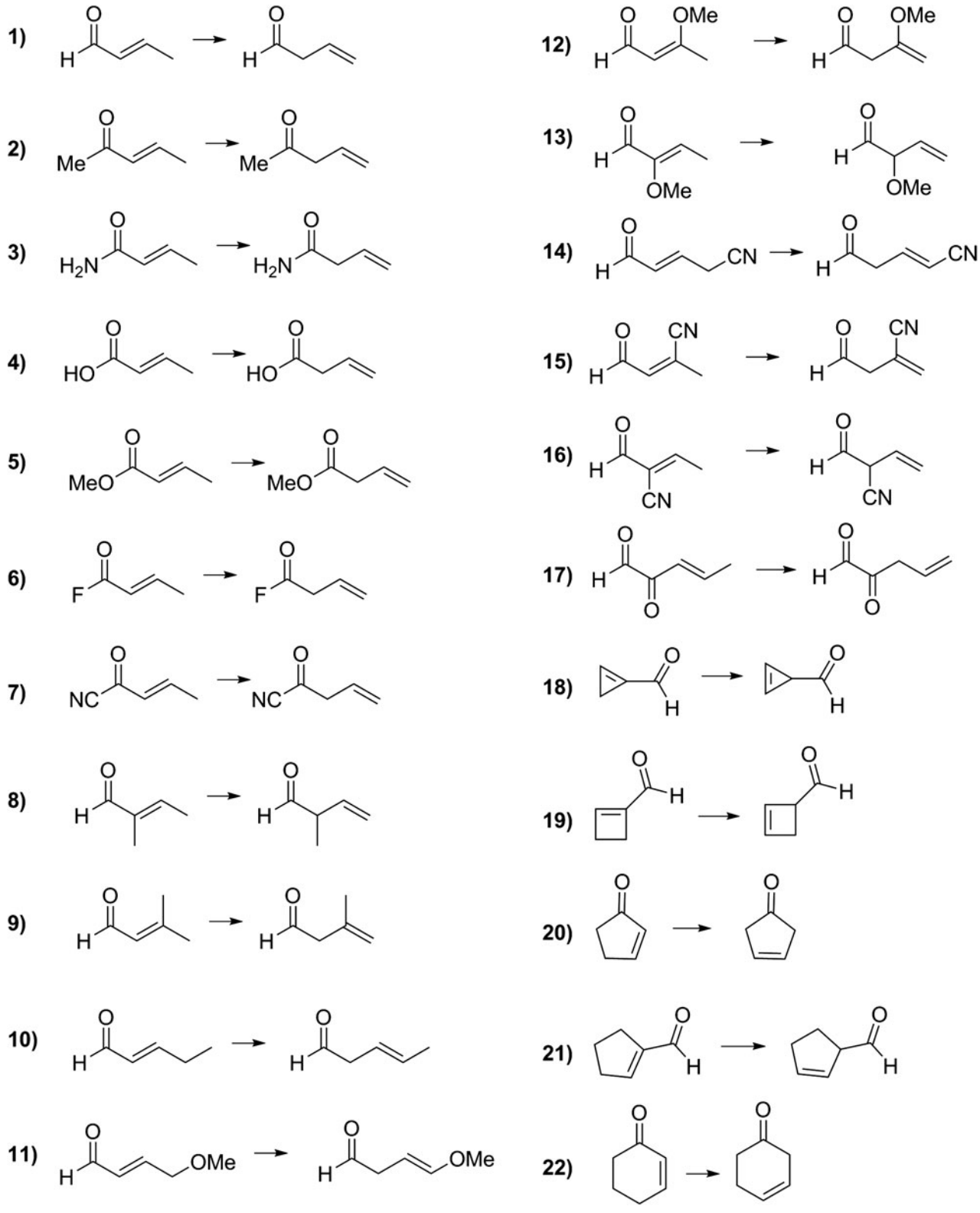

Figure 1. Isomerisation reactions in the EIE22 database.

Table 1. Component breakdown of the benchmark W1-F12 reaction energies (in kJ mol^{-1}) for the isomerisation reactions in the EIE22 database (shown in Figure 1).

Reaction	ΔSCF	ΔCCSD	Δ(T)	ΔCV[a]	ΔRel.[b]	ΔDBOC[c]	ΔZPVE[d]	ΔE_e[e]	ΔH_0[f]	$H_{298} - H_0$[g]	ΔH_{298}[f]
1	27.0	−2.0	1.8	0.1	0.0	0.01	−1.0	26.9	25.9	−0.1	25.8
2	17.6	−1.2	1.6	0.1	0.0	0.00	−0.4	18.1	17.7	−0.2	17.5
3	17.7	−4.4	0.3	0.2	0.0	−0.02	1.6	13.9	15.5	−1.0	14.4
4	18.8	−1.6	1.4	0.1	0.0	0.00	−0.4	18.7	18.3	0.0	18.3
5	18.5	−1.2	1.3	0.1	0.0	−0.01	−0.2	18.8	18.5	0.0	18.5
6	19.4	−1.9	1.5	0.1	0.0	0.00	−0.6	19.0	18.4	0.0	18.4
7	28.6	−2.0	1.8	0.2	0.0	0.01	0.0	28.5	28.5	0.0	28.5
8	30.1	1.1	2.0	0.4	0.0	0.03	0.0	33.6	33.5	−0.6	32.9
9	12.0	0.1	2.7	0.0	0.0	0.02	−0.1	14.9	14.8	−1.0	13.8
10	13.6	0.3	2.0	−0.1	0.0	0.01	−2.9	15.8	12.9	0.8	13.7
11	4.2	−3.6	0.1	−0.3	0.0	−0.06	−0.4	0.4	0.0	0.8	0.8
12	−3.1	3.3	4.3	−0.1	−0.1	−0.03	−1.3	4.4	3.1	−0.1	3.0
13	28.2	2.8	3.2	0.5	−0.1	0.00	−0.7	34.7	33.9	−0.6	33.3
14	4.4	−1.5	−0.2	−0.1	0.0	0.00	−1.0	2.6	1.7	0.2	1.9
15	16.7	1.7	2.3	0.1	0.0	0.02	−0.5	20.8	20.3	−0.3	19.9
16	39.1	−3.6	2.9	0.3	0.0	−0.01	−0.9	38.6	37.6	−0.1	37.6
17	22.0	−2.8	1.5	0.2	0.0	0.00	0.5	21.0	21.5	−0.4	21.1
18	−14.2	1.3	1.4	0.0	0.0	−0.07	−1.7	−11.5	−13.2	−0.4	−13.6
19	14.5	−1.8	1.2	0.2	0.0	−0.02	−0.6	14.1	13.5	0.0	13.6
20	18.0	−1.8	1.5	−0.2	0.0	−0.01	−2.2	17.5	15.4	0.1	15.5
21	21.6	−3.1	1.1	0.1	0.0	−0.02	−1.0	19.7	18.7	0.0	18.8
22	12.0	−0.4	1.6	−0.2	0.0	−0.02	−1.5	13.1	11.6	0.4	12.0

[a]Core-valence correction.
[b]Scalar-relativistic correction.
[c]Diagonal Born–Oppenheimer correction.
[d]ZPVE correction from B3LYP-D3/A′VTZ harmonic calculations (scaled by 0.99, see also Ref.[33]).
[e]Non-relativistic, all-electron, vibrationless, DBOC-exclusive CCSD(T) basis-set limit reference isomerisation energies (these are used for the evaluation of the DFT, composite, and *ab initio* procedures).
[f]Relativistic, all-electron, ZPVE-inclusive, DBOC-inclusive CCSD(T) basis-set limit reference isomerisation energies at 0 and 298 K (for comparison with experiment).
[g]Enthalpy functions ($H_{298} - H_0$) are obtained within the rigid rotor-harmonic oscillator approximation from the B3LYP-D3/A′VTZ calculated geometry and harmonic frequencies.

experimental value (−136 kJ mol^{-1}) by as much as 14 kJ mol^{-1}, however we note that the experimental value is not associated with an error bar. This suggests that re-examination of the experimental data for this compound may be in order.

A brief mention is warranted as to the magnitude and general effect of substituents on the isomerisation enthalpies for the reactions in the EIE22 database (see Figure 1 and Equation (1)). We begin by noting that for the 22 systems considered, the ΔH_{298} values range from −13.6 (**18**) to + 37.6 (**16**) kJ mol^{-1}, with 18 of the systems having ΔH_{298} values that are ≥ 12.0 kJ mol^{-1}, demonstrating the general favourability of the α,β-isomers vs. their β,γ-derivatives, a result that can be attributed, for the most part, to the existence of stabilising $\pi_{(C=C)} \rightarrow \pi^*_{(C=O)}$ orbital interactions in the former. Only one system, **18**, was associated with an exothermic ΔH_{298} value (−13.6 kJ mol^{-1}). The largest isomerisation energy is associated with system **16** (ΔH_{298} = 37.6 kJ mol^{-1}), and may reflect, in part, the loss of a double resonance stabilisation effect (ene-nitrile and ene-carbonyl) on going from the α,β- to β,γ-isomer.

We note that systems **11**, **12**, and **14** are associated with ΔH_{298} values that are close to thermo-neutral, with ΔH_{298} values of 0.8, 3.0, and 1.9 kJ mol^{-1}, respectively. The particularly small energy separation in system **11** ($\Delta H_{298} = 0.8$ kJ mol^{-1}) may be taken to imply that the stabilising $\pi_{(C=C)}$ to $\pi^*_{(C=O)}$ interaction lost in the α,β-isomer is balanced by the stabilising $LP_{(O)} \rightarrow \pi^*_{(C=C)}$ interaction formed in the β,γ-isomer. Similarly, the small energy difference in system **14** (ΔH_{298} = 1.9 kJ mol^{-1}) may indicate that the energetics associated with conjugative carbonyl-ene stabilisation in the α,β-isomer are of comparable magnitude to conjugative nitrile-ene stabilisation in the β,γ-isomer.

3.2. *Performance of DFT procedures for the isomerisation reactions in the EIE22 database*

The W1-F12 reaction energies (Table 1) provide a benchmark set of values that allows the evaluation of the performance of computationally less demanding procedures for the calculation of α,β- to β,γ-enecarbonyl isomerisation energies. For a rigorous comparison with the DFT data,

secondary effects that are not explicitly included in the DFT calculations, such as relativistic and ZPVE corrections, are excluded from the W1-F12 reference values. We begin by noting that all the isomerisation reactions in the EIE22 database conserve the numbers of each formal bond type and the number of C atoms in each hybridisation state on both sides of the reaction. In addition, some of the reactions also conserve the number of C atoms in each hapticity (i.e., primary, secondary, and tertiary). The use of transformations in which the chemical environments (except for π-conjugation) are largely balanced on the two sides of the reaction, allows us to evaluate the performance of approximate theoretical procedures for the calculation of the π-conjugation stabilisation energies in enecarbonyls.

It is well established that the performance of DFT can vary for different types of reactions. In particular, the accuracy of a given functional should increase as larger molecular fragments are conserved on the two sides of the reaction, due to an increasing degree of error cancelation between reactants and products. For example, it has been shown that the performance of DFT improves along the sequence: atomisation → isogyric → isodesmic → hypohomodesmotic → homodesmotic → hyperhomodesmotic reactions [17,24–29]. Since the performance of DFT functionals is expected to improve along this series, it is reasonable to tighten the criteria for recommending a DFT functional as the reaction hierarchy is traversed. In the following discussion, we will recommend DFT functionals that obtain an RMSD $\leq$ 2.1 kJ mol^{-1}, rather than the threshold of 'chemical accuracy' (i.e., RMSD $\leq$ 4.2 kJ mol^{-1}) that is usually used for atomisation and isogyric reactions. We also note that the reaction energies (ΔE_e) in the EIE22 data-set range between 0.4 and 38.6 kJ mol^{-1} (Table 1) and the average reaction energy is 18.8 kJ mol^{-1}, therefore an RMSD of ~10% of this average seems to be a reasonable threshold for recommending a DFT functional.

Table 2 gives the RMSD, MAD, mean signed deviation (MSD), and largest deviation (LD) from our benchmark W1-F12 results for the DFT functionals considered. Before proceeding to a detailed discussion of the performance of the families of functionals, we start by making the following general observations.

- With few exceptions, the GGA, MGGA, HGGA, and HMGGA functionals attain RMSDs above the threshold of 'chemical accuracy' (namely, RMSDs = 5.0–11.7 kJ mol^{-1}). The only two functionals that attain RMSDs below the threshold of 2.1 kJ mol^{-1} are M05-2X (RMSD = 2.1) and M06-2X (RMSD = 1.6 kJ mol^{-1}). We note that BMK-D3 also performs well with an RMSD of 2.7 kJ mol^{-1}.
- All the GGA, MGGA, HGGA, and HMGGA functionals tend to systematically overestimate the reactions energies, as evident from MSD ≈ MAD (with the notable exception of M06-HF).
- Where applicable, the inclusion of empirical D3 dispersion corrections systematically improve agreement with the W1-F12 results. However, the magnitude of these corrections is relatively modest ranging from 0.0 (B2GP-PLYP) to 1.1 (BLYP) kJ mol^{-1}.
- All of the RS functionals give good performance with RMSDs below the threshold of 'chemical accuracy'. In particular, ωB97, LC-ωPBE-D3, ωB97X, LC-ωPBE, and M11 show excellent performance with RMSDs = 1.4–2.3 kJ mol^{-1}.
- With the exception of B2K-PLYP, the double-hybrid DFT procedures give good performance with RMSDs ranging between 1.1 (DSD-BLYP) and 5.0 (B2-PLYP) kJ mol^{-1}. In particular, DSD-BLYP, B2GP-PLYP, and B2T-PLYP show excellent performance with RMSDs = 1.1–1.5 kJ mol^{-1}.

Of all the considered GGA functionals, the recently developed SOGGA11 procedure shows the best performance, with an RMSD of 5.6 kJ mol^{-1} and an LD of 11.2 kJ mol^{-1}. The rest of the GGA functionals exhibited notably poorer performance with RMSDs ranging from 8.5 (B97-D) to 10.9 (N12) kJ mol^{-1}. Note also that the LDs for these functionals vary between 15.4 and 18.9 kJ mol^{-1}. The inclusion of an empirical D3 dispersion correction was considered in the case of three functionals, namely BLYP, PBE, and BP86, and in all cases, resulted in a slight lowering of the RMSDs by amounts ranging from 0.6 (PBE-D3) to 1.1 (BLYP-D3) kJ mol^{-1}. It is instructive to compare the performance of the various DFT procedures across the EIE22 database vs. the DIE60 database [17]. Table S2 (Supplemental data) gathers the differences in RMSD (ΔRMSD = RMSD(EIE22) − RMSD(DIE60)). Inspection of the ΔRMSD values reveals that (with two exceptions) the performance of the GGA functionals deteriorates for the EIE22 test set, with the ΔRMSDs adopting positive values ranging from 0.5 (PBE) to 2.1 (BLYP-D3) kJ mol^{-1}. This indicates a greater difficulty of the considered GGAs in describing enecarbonyl vs. diene isomerisation energies. The two exceptions are HCTH407 and SOGGA11, where the RMSDs for the EIE22 set are 1.6 and 3.7 kJ mol^{-1} lower than for the DIE60 database, respectively. We additionally wish to note the remarkable 9.4 kJ mol^{-1} reduction in LD in the case of SOGGA11.

We now turn our attention to the MGGA functionals which sit one rung above the GGAs on Jacob's ladder. Inclusion of the kinetic energy density in these functionals does not offer improved performance over the GGAs. In fact, whereas SOGGA11 offered an RMSD of 5.6 kJ mol^{-1}, the best MGGA procedures give RMSDs of 9.3 (M11-L) and 9.4 (TPSS-D3) kJ mol^{-1}. The worst performing MGGA functionals are VSXC and M06-L with RMSDs of 11.5 and 11.7 kJ mol^{-1}, respectively. When comparing the performance of the MGGAs across the EIE22 vs. DIE60 data-sets, the ΔRMSDs indicate that most of the MGGAs

Table 2. Statistical analysis for the performance of DFT procedures for the calculation of the enecarbonyl isomerisation energies in the EIE22 database (in kJ mol^{-1})[a,b]

Type[c]	Method	RMSD	MAD	MSD	LD[d]
GGA	BLYP	9.8	9.1	9.1	16.5 (**16**)
	BLYP-D3	8.7	7.8	7.8	16.2 (**12**)
	B97-D	8.5	7.7	7.7	15.4 (**16**)
	HCTH407	9.7	8.7	8.6	17.8 (**16**)
	PBE	9.9	8.8	8.8	16.9 (**13**)
	PBE-D3	9.3	8.3	8.2	16.3 (**12**)
	BP86	10.1	9.1	9.1	16.7 (**13**)
	BP86-D3	9.2	8.1	8.0	16.7 (**12**)
	BPW91	10.3	9.2	9.2	17.3 (**16**)
	SOGGA11	5.6	4.9	4.3	11.2 (**16**)
	N12	10.9	9.7	9.7	18.9 (**13**)
MGGA	M06-L	11.7	10.5	10.4	21.4 (**13**)
	TPSS	10.2	9.4	9.4	16.7 (**16**)
	TPSS-D3	9.4	8.6	8.6	16.5 (**12**)
	τ-HCTH	10.5	9.4	9.4	18.0 (**16**)
	VSXC	11.5	10.3	10.1	21.6 (**8**)
	BB95	10.0	8.9	8.9	17.6 (**13**)
	M11-L	9.3	8.4	8.4	16.2 (**16**)
	MN12-L	10.7	9.8	9.8	18.8 (**13**)
HGGA	BH&HLYP	4.4	4.0	4.0	7.7 (**16**)
	BH&HLYP-D3	3.5	3.3	3.3	6.4 (**16**)
	B3LYP	7.5	6.9	6.9	12.7 (**16**)
	B3LYP-D3	6.5	5.9	5.9	11.4 (**12**)
	B3P86	7.9	7.1	7.1	13.4 (**13**)
	B3PW91	7.7	6.9	6.9	13.3 (**16**)
	B3PW91-D3	6.7	5.9	5.8	11.9 (**13**)
	PBE0	6.9	6.1	6.1	12.0 (**13**)
	PBE0-D3	6.3	5.5	5.5	11.3 (**13**)
	B97-1	6.6	6.0	6.0	11.1 (**16**)
	B98	6.6	6.0	6.0	11.1 (**16**)
	X3LYP	7.2	6.6	6.6	12.1 (**16**)
	SOGGA11-X	5.0	4.5	4.5	8.5 (**16**)
HMGGA	M05	5.8	4.9	4.7	11.0 (**16**)
	M05-2X	2.1	1.9	1.4	3.9 (**18**)
	M06	6.3	5.4	5.4	11.1 (**16**)
	M06-2X	1.6	1.4	1.0	2.7 (**18**)
	M06-HF	7.1	6.4	−6.2	11.9 (**13**)
	BMK	3.2	2.9	2.5	6.0 (**13**)
	BMK-D3	2.7	2.3	1.8	6.2 (**12**)
	B1B95	6.6	5.8	5.8	12.0 (**13**)
	B1B95-D3	5.9	5.2	5.1	11.3 (**13**)
	TPSSh	8.9	8.2	8.2	14.7 (**16**)
	τ-HCTHh	7.6	6.9	6.9	12.8 (**16**)
	PW6B95	6.2	5.6	5.6	10.8 (**13**)
	PW6B95-D3	5.9	5.3	5.3	10.5 (**13**)
RS	CAM-B3LYP	4.1	3.6	3.6	7.0 (**16**)
	CAM-B3LYP-D3	3.5	3.0	3.0	6.2 (**16**)
	LC-ωPBE	2.2	1.8	0.4	4.5 (**11**)
	LC-ωPBE-D3	1.8	1.3	−0.6	5.1 (**11**)
	ωB97	1.4	1.2	0.1	2.8 (**18**)
	ωB97X	2.1	1.8	1.3	3.6 (**17**)
	ωB97X-D	3.1	2.7	2.5	6.0 (**16**)
	M11	2.3	1.9	0.3	4.7 (**18**)

Table 2. (Continued)

Type[c]	Method	RMSD	MAD	MSD	LD[d]
DH	B2-PLYP	5.0	4.7	4.7	8.1 (**16**)
	B2-PLYP-D3	4.4	4.0	4.0	8.2 (**12**)
	B2GP-PLYP	1.3	0.8	0.1	4.0 (**13**)
	B2GP-PLYP-D3	1.3	0.8	−0.2	4.2 (**13**)
	B2K-PLYP	12.4	9.7	7.3	30.0 (**12**)
	B2T-PLYP	1.5	0.9	−0.1	5.1 (**13**)
	DSD-BLYP	1.1	0.9	0.4	2.9 (**13**)
	DSD-PBEP86	2.9	2.7	2.7	4.6 (**13**)
	DSD-PBEP86-D3	2.7	2.5	2.5	4.6 (**13**)
	PWPB95	3.9	3.5	3.5	7.0 (**13**)
	PWPB95-D3	3.7	3.3	3.3	6.8 (**13**)

[a]The standard DFT calculations were carried out in conjunction with the A′VTZ basis set, while the DHDFT calculations, which exhibit slower basis-set convergence, were carried out in conjunction with the A′VQZ basis set.
[b]RMSD = root mean square deviation, MAD = mean absolute deviation, MSD = mean signed deviation, LD = largest deviation (in absolute value).
[c]GGA = generalised gradient approximation, HGGA = hybrid-GGA, MGGA = meta-GGA, RS = range-separated HGGA, HMGGA = hybrid-meta-GGA, DH = double hybrid.
[d]The reaction numbers are given in parenthesis (see Figure 1).

perform worse across the former set, with the largest deterioration in performance being noted in the case of VSXC (1.6 kJ mol^{-1}). Two procedures, τ-HCTH and M11-L show slight improvements by 0.3 and 0.6 kJ mol^{-1}, respectively (Table S2, Supplemental data).

The HGGAs are generally superior to the GGAs and MGGAs with RMSDs ranging between 3.5 (BH&HLYP-D3) and 7.9 (B3P86) kJ mol^{-1}. We note that reaction **16** poses a particular challenge for the majority of HGGA procedures, namely eight out of thirteen, with LDs ranging from 6.4 (BH&HLYP-D3) to 13.3 (B3PW91) kJ mol^{-1}. As for a comparison between the performance of the HGGAs across the EIE22 vs. DIE60 data-sets, over half of the functionals perform worse on the former, with most of the ΔRMSDs ranging from 0.8 (B97-1) to 1.2 (B3LYP-D3) kJ mol^{-1}, whilst those that performed better did so by amounts ranging from 0.1 (BH&HLYP) to 0.6 (SOGGA11-X) kJ mol^{-1} (Table S2, Supplemental data).

The RMSDs of the HMGGA procedures span a wide range from 1.6 (M06-2X) up to 8.9 (TPSSh) kJ mol^{-1}. Inspection of Table 2 reveals that the optimal percentage of Hartree–Fock-type exchange seems to be around ∼50%. For example, M06-2X and M05-2X (54% and 56% of exact exchange, respectively) are the best performing methods with RMSDs of 1.6 and 2.1 kJ mol^{-1}, respectively. Similarly, BMK-D3 and BMK (42% of exact exchange) give somewhat higher RMSDs of 2.7 and 3.2 kJ mol^{-1}, respectively. However, functionals with 25%–30% of Hartree–Fock exchange, such as M05, M06, PW6B95, and B1B95 give significantly higher RMSDs of 5.8–6.6 kJ mol^{-1} (see also discussion in Ref. [17]). We also note that whilst M06-HF with 100% Hartree–Fock exchange gives an even higher RMSD of 7.1 kJ mol^{-1}, Hartree–Fock theory by itself gives a similar performance to BMK with an RMSD of 2.9 kJ mol^{-1} (see also discussion in Section 3.3). We note that the good performance of the HGGAs and HMGGAs with ∼50% of Hartree–Fock exchange indicates that the self-interaction error (also known as the delocalisation error) [112] may play an important role in these systems. This is also indicated by the generally good performance of the RS functionals (*vide infra*).

The RS hybrid-GGAs give very good performance with RMSDs ranging from 1.4 (ωB97) to 4.1 (CAM-B3LYP) kJ mol^{-1}. We note that the superb performance of ωB97 is followed closely by LC-ωPBE-D3, with RMSD = 1.8 kJ mol^{-1}. Comparing the performance of the RS functionals for their accuracy across the EIE22 vs. DIE60 sets, we find that six of the eight functionals offer modest to substantial improvements in the RMSDs, ranging from 0.3 (ωB97X-D) to 3.0 (LC-ωPBE-D3) kJ mol^{-1}. However, a more striking result is that the LDs are reduced by amounts ranging from 1.4 (CAM-B3LYP-D3) to 7.7 (LC-ωPBE) kJ mol^{-1} (Table S2, Supplemental data).

The double-hybrid functionals show good performance with RMSDs ranging between 1.1 (DSD-BLYP) and 5.0 (B2-PLYP) kJ mol^{-1}. We note that B2GP-PLYP gives similar performance to DSD-BLYP with an RMSD of 1.3 kJ mol^{-1}, and that both procedures attain near-zero MSDs (0.1 and 0.4 kJ mol^{-1}, respectively). Finally, we note that B2K-PLYP, which was parameterised for thermochemical kinetics, shows very poor performance with an RMSD of 12.4 kJ mol^{-1} (this is consistent with B2K-PLYP's poor performance for the DIE60 database) [86,87].

Table S4 (Supplemental data) gives an overview of the basis-set convergence for the reactions in the EIE22 database. We consider Dunning's A′V*n*Z basis sets (n = D, T, and Q). With few exceptions, the functionals converge relatively smoothly and rapidly to the basis-set limit

Table 3. Statistical analysis for the performance of composite and standard *ab initio* methods for the calculation of the enecarbonyl isomerisation energies in the EIE22 database (in kJ mol^{-1})[a].

Basis set	Methods	RMSD	MAD	MSD	LD
	G3	1.0	0.8	−0.6	2.3 (**3**)
	G3(MP2)	1.6	1.5	−1.3	2.6 (**13**)
	G3B3	1.4	1.2	−1.0	2.6 (**13**)
	G3(MP2)B3	2.1	1.9	−1.7	3.8 (**13**)
	G4	1.8	1.4	−1.2	3.7 (**13**)
	G4(MP2)	2.3	2.1	−1.9	4.8 (**13**)
	G4(MP2)-6X	1.5	1.3	−1.1	3.6 (**13**)
	CBS-QB3	1.2	1.0	−0.9	2.4 (**13**)
	CBS-APNO	1.0	0.7	−0.4	3.0 (**3**)
A′VQZ	HF	2.9	2.1	−0.8	7.6 (**12**)
	MP2	2.0	1.8	1.7	3.6 (**13**)
	SCS-MP2	0.8	0.7	0.1	1.5 (**12**)
	MP2.5	0.6	0.5	0.3	1.1 (**15**)
	MP3	1.6	1.3	−1.1	4.3 (**12**)
	SCS-MP3	1.0	0.8	−0.2	2.4 (**12**)
A′VTZ	HF	2.9	2.1	−0.6	7.4 (**12**)
	MP2	2.0	1.8	1.8	3.2 (**13**)
	SCS-MP2	1.0	0.8	0.2	1.8 (**18**)
	MP2.5	0.6	0.5	0.3	1.3 (**21**)
	MP3	1.6	1.4	−1.1	4.0 (**12**)
	SCS-MP3	1.1	0.9	−0.2	2.1 (**12**)
	MP4	1.4	1.2	1.2	2.9 (**12**)
	CCSD	2.2	1.9	−1.8	4.5 (**13**)
	SCS-CCSD	2.9	2.6	−2.5	4.9 (**16**)
	SCS(MI)CCSD	1.7	1.5	−1.5	3.1 (**13**)
	CCSD(T)	0.6	0.4	−0.1	1.4 (**13**)
	CCSD(T)/CBS[b]	0.7	0.6	−0.6	1.4 (**8**)
A′VDZ	HF	3.1	2.2	−0.6	7.3 (**13**)
	MP2	2.0	1.9	1.8	3.6 (**12**)
	SCS-MP2	1.4	1.2	0.2	2.9 (**18**)
	MP2.5	1.1	0.9	0.3	2.0 (**11**)
	MP3	2.1	1.8	−1.2	3.9 (**12**)
	SCS-MP3	1.6	1.3	−0.2	2.8 (**13**)
	MP4	1.4	1.2	0.9	3.3 (**18**)
	CCSD	2.8	2.4	−2.1	6.3 (**13**)
	SCS-CCSD	3.6	3.1	−2.8	6.9 (**13**)
	SCS(MI)CCSD	2.4	2.1	−1.8	5.1 (**13**)
	CCSD(T)	1.5	1.1	−0.4	3.4 (**13**)

[a]Footnotes b and d to Table 2 apply here.
[b]CCSD(T)/CBS ≈ CCSD(T)/A′VDZ + MP2/A′V{T,Q}Z − MP2/A′VDZ.

such that even the A′VDZ basis set gives acceptable results. For example, the RMSDs obtained with the A′VDZ basis set are generally higher by 0.1–0.5 kJ mol^{-1} than those obtained with A′VQZ basis set, and those obtained with the A′VTZ are generally higher by 0.1–0.3 kJ mol^{-1} than those obtained with A′VQZ basis set. Finally, we note that the SOGGA11 functional exhibits a more pronounced (and somewhat erratic) basis-set dependence, namely we obtain the following RMSDs: 8.4 (A′VDZ), 4.4 (A′VTZ), and 5.6 (A′VQZ) kJ mol^{-1} (Table S4, Supplemental data). In response to a reviewer's inquiry, we have also evaluated the performance of the SOGGA11 functional in conjunction with the A′V5Z basis set. Interestingly, we obtain an RMSD of 8.2 kJ mol^{-1} for the SOGGA11/A′V5Z level of theory, again indicating a relatively strong basis-set dependence for this functional.

3.3. Performance of composite and standard ab initio procedures for the isomerisation reactions in the EIE22 database

Table 3 gives an overview of the performance of the composite G3, G3(MP2), G3B3, G3(MP2)B3, G4, G4(MP2), G4(MP2)-6X, CBS-QB3, and CBS-APNO procedures, as

well as several *ab initio* methods (e.g., MP2, MP2.5, MP3, MP4, SCS-MP2, SCS-MP3, CCSD, and CCSD(T)). It is clear that the composite procedures do not have difficulty with the reactions in the EIE22 data-set. All of the composite procedures are associated with RMSDs below 2.3 kJ mol^{-1}. Of the G4-type procedures, G4(MP2)-6X, which has the same computational cost as G4(MP2) gives the best performance with an RMSD of 1.5 kJ mol^{-1}. The G4 and G4(MP2) procedures give slightly larger RMSDs of 1.8 and 2.3 kJ mol^{-1}, respectively. Of the G3-type procedures, G3 and G3B3 give the best performance with RMSDs of 1.0 and 1.4 kJ mol^{-1}, respectively. The CBS-type procedures show similar performance to G3 and G3B3, with RMSDs of 1.0 (CBS-APNO) and 1.2 (CBS-QB3) kJ mol^{-1}, respectively.

We now turn our attention to the performance of the standard wavefunction methods in conjunction with the A′V*n*Z basis sets (n = D, T, and Q) (Table 3). We start by noting that practically all the *ab initio* methods converge fairly rapidly to the basis-set limit. For example, for the methods for which we have both A′VTZ and A′VQZ results (HF, MP2, SCS-MP2, MP2.5, MP3, and SCS-MP3), the difference in RMSDs between the two basis sets vary between 0.0 and 0.2 kJ mol^{-1}. In the following discussion, we will use the results obtained with the A′VQZ basis set for the abovementioned methods, and the A′VTZ basis set for all the rest. Nevertheless, it is worth mentioning that even the A′VDZ basis set does not perform too badly, considering its low computational cost. Specifically, the difference in the overall RMSDs between the A′VTZ and A′VDZ basis sets range from 0.2 (HF) to 0.9 (CCSD(T)) kJ mol^{-1} (Table 3). As mentioned in Section 3.2, HF theory gives a relatively good performance (RMSD = 2.9 kJ mol^{-1}) and actually outperforms all of the considered GGA, MGGA, HGGA, and 10 of the 13 HMGGA functionals. The DFT functionals that consistently outperform HF theory are the RS procedures (except CAM-B3LYP and its D3-corrected analogue), and the HMGGAs with ∼50% of exact exchange (e.g., M05-2X and M06-2X). Second-order Møller–Plesset perturbation theory (MP2) results in an RMSD of 2.0 kJ mol^{-1}, whilst this is reduced to just 0.8 kJ mol^{-1} when the same-spin and opposite-spin components of the MP2 correlation energy are scaled, as in the SCS-MP2 procedure. Inclusion of higher order excitations in procedures such as MP2.5, MP3, SCS-MP3, and MP4 results in RMSDs ranging between 0.6 and 1.6 kJ mol^{-1}. Thus, the increase in the computational cost (relative to SCS-MP2) does not seem to warrant their use. The CCSD method attains a somewhat disappointing RMSD of 2.2 kJ mol^{-1}, whilst SCS-CCSD is worse (2.9 kJ mol^{-1}) and SCS(MI)CCSD is better (1.7 kJ mol^{-1}). The CCSD(T) method attains RMSDs of 0.6 and 1.5 kJ mol^{-1} in conjunction with the A′VTZ and A′VDZ basis sets, respectively. It is of interest to assess the performance of the CCSD(T) method using an additivity-based approach in which the CCSD(T)/CBS energy is estimated from the CCSD(T)/A′VDZ energy and an MP2-based basis-set-correction term (ΔMP2 = MP2/A′V{T,Q}Z − MP2/A′VDZ, where the MP2/A′V{T,Q}Z energy is extrapolated to the basis-set limit with an extrapolation exponent of 3) [113]. This cost-effective approach, has been shown to give slightly better performance than the CCSD(T)/cc-pVTZ level of theory for the DIE60 database [17]. However, here it results in an RMSD of 0.7 kJ mol^{-1}, which is slightly worse than standard CCSD(T) with the A′VTZ basis set (RMSD = 0.6 kJ mol^{-1}).

4. Conclusions

We obtain benchmark α,β- to β,γ-enecarbonyl isomerisation energies, for a diverse set of 22 systems, by means of the high-level W1-F12 composite thermochemistry protocol. We use these benchmark energies (a.k.a. the EIE22 database) to evaluate the performance of a variety of contemporary DFT and *ab initio* procedures for the calculation of enecarbonyl π-conjugation stabilisation energies. With regard to the performance of the DFT and DHDFT procedures across the EIE22 database, we make the following observations.

- It is evident that the calculation of π-delocalisation energies represents a general problem for conventional DFT methods that is not limited to diolefin systems (as previously shown in Ref. [17]) but is also extended to enecarbonyl systems in which heteroatoms (O and N) are part of the conjugated π-system.
- With the exception of four functionals (M05-2X, M06-2X, BMK, and BH&HLYP), all the conventional DFT procedures result in RMSDs of 5.0–11.7 kJ mol^{-1} (note that by conventional DFT procedures we refer to all the GGA, MGGA, HGGA, and HMGGA functionals). The best performing functionals are M05-2X and M06-2X with RMSDs of 2.1 and 1.6 kJ mol^{-1}, respectively.
- The considered GGA and MGGA functionals give poor performance with RMSDs ranging between 8.5 (B97-D) and 11.7 (M06-L) kJ mol^{-1}, with the exception of SOGGA11 which gives an RMSD of 5.6 kJ mol^{-1}.
- The HGGAs show better performance with RMSDs ranging between 3.5 (BH&HLYP-D3) and 7.9 (B3P86) kJ mol^{-1}. Note that the popular B3LYP functional gives RMSDs of 6.5 and 7.5 kJ mol^{-1} with and without the dispersion D3 correction, respectively.
- The RMSDs of the HMGGA procedures span a wide range from 1.6 (M06-2X) to 8.9 (TPSSh) kJ mol^{-1}. Apart from M06-2X, the M05-2X functional also shows very good performance with an RMSD of 2.1 kJ mol^{-1}. We also note the fairly good performance

of BMK (RMSD = 2.7 and 3.2 kJ mol^{-1}, with and without the D3 dispersion correction, respectively). All the other HMGGAs give RMSDs $\geq$ 5.8 kJ mol^{-1}.
- The RS procedures give good performance with RMSDs varying between 1.4 (ωB97) and 4.1 (CAM-B3LYP) kJ mol^{-1}. We also note the very good performance of the LC-ωPBE-D3 (RMSD = 1.8 kJ mol^{-1}) and ωB97X-D (RMSD = 2.1 kJ mol^{-1}) functionals.
- As expected, the double-hybrid procedures give good performance, the best performing functionals are: DSD-BLYP (1.1) and B2GP-PLYP (1.3 kJ mol^{-1}).

With regard to the performance of the composite and standard *ab initio* procedures, we draw the following conclusions.

- The composite procedures show excellent performance with RMSDs ranging between 1.0 (G3 and CBS-APNO) and 2.3 (G4(MP2)) kJ mol^{-1}.
- The standard *ab initio* procedures also show good performance with SCS-MP2 offering the best performance-to-computational cost ratio with an RMSD of 1.0 and 1.4 kJ mol^{-1}, in conjunction with the A′VTZ and A′VDZ basis sets, respectively.

Acknowledgements

We gratefully acknowledge the generous allocation of computing time from the National Computational Infrastructure (NCI) National Facility, and the support of iVEC through the use of advanced computing resources located at iVEC@UWA, the provision of an International Postgraduate Research Scholarship (to Li-Juan Yu), and an Australian Research Council (ARC) Discovery Early Career Researcher Award (to Amir Karton, project number: DE140100311).

Supplemental data

Supplemental data for this article can be accessed here.

References

[1] K. Natarajan, S. Singh, T.R. Burke, Jr., D. Grunberger, and B.B. Aggarwal, Proc. Natl. Acad. Sci. U.S.A **93**, 9090 (1996).
[2] J.W. Han, B.G. Lee, Y.K. Kim, J.W. Yoon, H.K. Jin, S. Hong, H.Y. Lee, K.R. Lee, and H.W. Lee, Br. J. Pharmacology **133**, 503 (2001).
[3] P.V. Ramachandran, M. Yip-Schneider, and C.M. Schmidt, Future Medicinal Chem. **1**, 179 (2009).
[4] A. Chariot, Biochem. Pharmacology **72**, 1051 (2006).
[5] P. Schreier, F. Drawert, and A. Junker, J. Agric. Food Chem. **24**, 331 (1976).
[6] G.R. Takeoka, R.A. Flath, M. Güntert, and W. Jennings, J. Agric. Food Chem. **36**, 553 (1988).
[7] K. Bloch, Acc. Chem. Res. **2**, 193 (1969).
[8] J.B. Jones, and D.C. Wigfield, Can. J. Chem. **47**, 4459 (1969).
[9] P. Talalay, Ann. Rev. Biochem. **34**, 347 (1965).
[10] R.L. Cargill, and J.W. Crawford, J. Org. Chem. **35**, 356 (1970).
[11] R.M. Pollack, and R.H. Kayser, J. Am. Chem. Soc. **98**, 4174 (1976).
[12] R.H. Kayser, and R.M. Pollack, J. Am. Chem. Soc. **97**, 952 (1975).
[13] Y. Dai, X. Feng, H. Liu, H. Jiang, and M. Bao, J. Org. Chem. **76**, 10068 (2011).
[14] L.-G. Zhuo, Z.-K. Yao, and Z.-X. Yu, Org. Lett. **15**, 4634 (2013).
[15] G.A.R. Kon, and K.S. Nargund, J. Chem. Soc. 623 (1934).
[16] T. Sugita, K. Gohda, and T. Kagiya, Bull. Chem. Soc. Jpn. **63**, 278 (1990).
[17] L.-J. Yu, and A. Karton, Chem. Phys. **441**, 166 (2014).
[18] A. Karton, and J.M.L. Martin, J. Chem. Phys. **136**, 124114 (2012).
[19] H.-J. Werner, P.J. Knowles, G. Knizia, F.R. Manby, M. Schütz, P. Celani, T. Korona, R. Lindh, A. Mitrushenkov, G. Rauhut, K.R. Shamasundar, T.B. Adler, R.D. Amos, A. Bernhardsson, A. Berning, D.L. Cooper, M.J.O. Deegan, A.J. Dobbyn, F. Eckert, E. Goll, C. Hampel, A. Hesselmann, G. Hetzer, T. Hrenar, G. Jansen, C. Köppl, Y. Liu, A.W. Lloyd, R.A. Mata, A.J. May, S.J. McNicholas, W. Meyer, M.E. Mura, A. Nicklaß, D.P. O'Neill, P. Palmieri, D. Peng, K. Pflüger, R. Pitzer, M. Reiher, T. Shiozaki, H. Stoll, A.J. Stone, R. Tarroni, T. Thorsteinsson, M. Wang, MOLPRO is a package of ab initio programs. MOLPRO, version 2012.1. <http:www.molpro.net>.
[20] J.M.L. Martin, and G. Oliveira, J. Chem. Phys. **111**, 1843 (1999).
[21] A. Karton, E. Rabinovich, J.M.L. Martin, and B. Ruscic, J. Chem. Phys. **125**, 144108 (2006).
[22] K.A. Peterson, D. Feller, and D.A. Dixon, Theor. Chem. Acc. **131**, 1079 (2012).
[23] T. Helgaker, W. Klopper, and D.P. Tew, Mol. Phys. **106**, 2107 (2008).
[24] A. Karton, S. Daon, and J.M.L. Martin, Chem. Phys. Lett. **510**, 165 (2011).
[25] S.E. Wheeler, K.N. Houk, P.V.R. Schleyer, and W.D. Allen, J. Am. Chem. Soc. **131**, 2547 (2009).
[26] S.E. Wheeler, WIREs Comput. Mol. Sci. **2**, 204 (2012).
[27] R.O. Ramabhadran, and K. Raghavachari, J. Phys. Chem. A **116**, 7531 (2012).
[28] R.O. Ramabhadran, and K. Raghavachari, J. Chem. Theory Comput. **7**, 2094 (2011).
[29] A. Karton, D. Gruzman, and J.M.L. Martin, J. Phys. Chem. A **113**, 8434 (2009).
[30] C. Hättig, W. Klopper, A. Köhn, and D.P. Tew, Chem. Rev. **112**, 4 (2012).
[31] K.A. Peterson, T.B. Adler, and H.-J. Werner, J. Chem. Phys. **128**, 084102 (2008).
[32] J.G. Hill, K.A. Peterson, G. Knizia, and H.-J. Werner, J. Chem. Phys. **131**, 194105 (2009).
[33] A. Karton, L.-J. Yu, M.K. Kesharwani, and J.M.L. Martin, Theor. Chem. Acc. **133**, 1483 (2014).
[34] J. Noga, S. Kedžuch, and J. Šimunek, J. Chem. Phys. **127**, 034106 (2007).
[35] G. Knizia, and H.-J. Werner, J. Chem. Phys. **128**, 154103 (2008).
[36] T.B. Adler, G. Knizia, and H.-J. Werner, J. Chem. Phys. **127**, 221106 (2007).
[37] T.H. Dunning, J. Chem. Phys. **90**, 1007 (1989).
[38] R.A. Kendall, T.H. Dunning, and R.J. Harrison, J. Chem. Phys. **96**, 6796 (1992).

[39] S. Ten-no, and J. Noga, WIREs Comput. Mol. Sci. **2**, 114 (2012).
[40] S. Ten-no, Chem. Phys. Lett. **398**, 56 (2004).
[41] H.-J. Werner, T.B. Adler, and F.R. Manby, J. Chem. Phys. **126**, 164102 (2007).
[42] G. Knizia, T.B. Adler, and H.-J. Werner, J. Chem. Phys. **130**, 054104 (2009).
[43] K.A. Peterson, and T.H. Dunning, J. Chem. Phys. **117**, 10548 (2002).
[44] M. Douglas, and N.M. Kroll, Ann. Phys. **82**, 89 (1974).
[45] B.A. Hess, Phys. Rev. A **33**, 3742 (1986).
[46] W.A. de Jong, R.J. Harrison, and D.A. Dixon, J. Chem. Phys. **114**, 48 (2001).
[47] J.F. Stanton, J. Gauss, M.E. Harding, and P.G. Szalay, with contributions from A.A. Auer, R.J. Bartlett, U. Benedikt, C. Berger, D.E. Bernholdt, Y.J. Bomble, L. Cheng, O. Christiansen, M. Heckert, O. Heun, C. Huber, T.-C. Jagau, D. Jonsson, J. Jusélius, K. Klein, W.J. Lauderdale, D.A. Matthews, T. Metzroth, L.A. Mück, D.P. O'Neill, D.R. Price, E. Prochnow, C. Puzzarini, K. Ruud, F. Schiffmann, W. Schwalbach, C. Simmons, S. Stopkowicz, A. Tajti, J. Vázquez, F. Wang, J.D. Watts and the integral packages MOLECULE (J. Almlöf and P.R. Taylor), PROPS (P.R. Taylor), ABACUS (T. Helgaker, H.J. Aa. Jensen, P. Jørgensen, and J. Olsen), and ECP routines by A.V. Mitin and C. van Wüllen, CFOUR, a quantum chemical program package. <http://www.cfour.de>.
[48] A. Karton, and J.M.L. Martin, J. Chem. Phys. **133**, 144102 (2010).
[49] C. Lee, W. Yang, and R.G. Parr, Phys. Rev. B **37**, 785 (1988).
[50] A.D. Becke, J. Chem. Phys. **98**, 5648 (1993).
[51] P.J. Stephens, F.J. Devlin, C.F. Chabalowski, and M.J. Frisch, J. Phys. Chem. **98**, 11623 (1994).
[52] S. Grimme, S. Ehrlich, and L. Goerigk, J. Comput. Chem. **32**, 1456 (2011).
[53] S. Grimme, J. Antony, S. Ehrlich, and H. Krieg, J. Chem. Phys. **132**, 154104 (2010).
[54] S. Grimme, WIREs Comput. Mol. Sci. **1**, 211 (2011).
[55] A.D. Becke, and E.R. Johnson, J. Chem. Phys. **123**, 154101 (2005).
[56] M.J. Frisch, G.W. Trucks, H.B. Schlegel, G.E. Scuseria, M.A. Robb, J.R. Cheeseman, G. Scalmani, V. Barone, B. Mennucci, G.A. Petersson, H. Nakatsuji, M. Caricato, X. Li, H.P. Hratchian, A.F. Izmaylov, J. Bloino, G. Zheng, J.L. Sonnenberg, M. Hada, M. Ehara, K. Toyota, R. Fukuda, J. Hasegawa, M. Ishida, T. Nakajima, Y. Honda, O. Kitao, H. Nakai, T. Vreven, J.A. Montgomery, Jr., J.E. Peralta, F. Ogliaro, M. Bearpark, J.J. Heyd, E. Brothers, K.N. Kudin, V.N. Staroverov, R. Kobayashi, J. Normand, K. Raghavachari, A. Rendell, J.C. Burant, S.S. Iyengar, J. Tomasi, M. Cossi, N. Rega, J.M. Millam, M. Klene, J.E. Knox, J.B. Cross, V. Bakken, C. Adamo, J. Jaramillo, R. Gomperts, R.E. Stratmann, O. Yazyev, A.J. Austin, R. Cammi, C. Pomelli, J.W. Ochterski, R.L. Martin, K. Morokuma, V.G. Zakrzewski, G.A. Voth, P. Salvador, J.J. Dannenberg, S. Dapprich, A.D. Daniels, Ö. Farkas, J.B. Foresman, J.V. Ortiz, J. Cioslowski, and D.J. Fox, *Gaussian 09, Revision D.01* (Gaussian, Inc., Wallingford CT, 2009).
[57] J.P. Perdew, A. Ruzsinszky, J. Tao, V.N. Staroverov, G.E. Scuseria, and G.I. Csonka, J. Chem. Phys. **123**, 062201 (2005).
[58] A.D. Becke, Phys. Rev. A **38**, 3098 (1988).
[59] S. Grimme, J. Comp. Chem. **27**, 1787 (2006).
[60] A.D. Boese, and N.C. Handy, J. Chem. Phys. **114**, 5497 (2001).
[61] J.P. Perdew, K. Burke, and M. Ernzerhof, Phys. Rev. Lett. **77**, 3865 (1996); *ibid*. **78**, 1396 (1997).
[62] J.P. Perdew, Phys. Rev. B **33**, 8822 (1986).
[63] J.P. Perdew, J.A. Chevary, S.H. Vosko, K.A. Jackson, M.R. Pederson, D.J. Singh, and C. Fiolhais, Phys. Rev. B **46**, 6671 (1992).
[64] R. Peverati, Y. Zhao, and D.G. Truhlar, J. Phys. Chem. Lett. **2**, 1991 (2011).
[65] R. Peverati, and D.G. Truhlar, J. Chem. Theory Comput. **8**, 2310 (2012).
[66] Y. Zhao, and D.G. Truhlar, J. Chem. Phys. **125**, 194101 (2006).
[67] J.M. Tao, J.P. Perdew, V.N. Staroverov, and G.E. Scuseria, Phys. Rev. Lett. **91**, 146401 (2003).
[68] A.D. Boese, and N.C. Handy, J. Chem. Phys. **116**, 9559 (2002).
[69] T. van Voorhis, and G.E. Scuseria, J. Chem. Phys. **109**, 400 (1998).
[70] A.D. Becke, J. Chem. Phys. **104**, 1040 (1996).
[71] R. Peverati, and D.G. Truhlar, J. Phys. Chem. Lett. **3**, 117 (2012).
[72] R. Peverati, and D.G. Truhlar, Phys. Chem. Chem. Phys. **10**, 13171 (2012).
[73] A.D. Becke, J. Chem. Phys. **98**, 1372 (1993).
[74] C. Adamo, and V. Barone, J. Chem. Phys. **110**, 6158 (1999).
[75] F.A. Hamprecht, A.J. Cohen, D.J. Tozer, and N.C. Handy, J. Chem. Phys. **109**, 6264 (1998).
[76] H.L. Schmider, and A.D. Becke, J. Chem. Phys. **108**, 9624 (1998).
[77] X. Xu, Q. Zhang, R.P. Muller, and W.A. Goddard, J. Chem. Phys. **122**, 014105 (2005).
[78] R. Peverati, and D.G. Truhlar, J. Chem. Phys. **135**, 191102 (2011)
[79] Y. Zhao, N.E. Schultz, and D.G. Truhlar, J. Chem. Phys. **123**, 161103 (2005).
[80] Y. Zhao, N.E. Schultz, and D.G. Truhlar, J. Chem. Theory Comput. **2**, 364 (2006).
[81] Y. Zhao, and D.G. Truhlar, Theor. Chem. Acc. **120**, 215 (2008).
[82] A.D. Boese, and J.M.L. Martin, J. Chem. Phys. **121**, 3405 (2004).
[83] V.N. Staroverov, G.E. Scuseria, J. Tao, and J.P. Perdew, J. Chem. Phys. **119**, 12129 (2003).
[84] Y. Zhao, and D.G. Truhlar, J. Phys. Chem. A **109**, 5656 (2005).
[85] S. Grimme, J. Chem. Phys. **124**, 034108 (2006).
[86] A. Karton, A. Tarnopolsky, J.–F. Lamere, G.C. Schatz, and J.M.L. Martin, J. Phys. Chem. A **112**, 12868 (2008).
[87] A. Tarnopolsky, A. Karton, R. Sertchook, D. Vuzman, and J.M.L. Martin, J. Phys. Chem. A **112**, 3 (2008).
[88] S. Kozuch, D. Gruzman, and J.M.L. Martin, J. Phys. Chem. C **114**, 20801 (2010).
[89] S. Kozuch, and J.M.L. Martin, Phys. Chem. Chem. Phys. **13**, 20104 (2011).
[90] S. Kozuch, and J.M.L. Martin, J. Comput. Chem. **34**, 2327 (2013).
[91] L. Goerigk, and S. Grimme, J. Chem. Theory Comput. **7**, 291 (2011).
[92] T. Yanai, D. Tew, and N. Handy, Chem. Phys. Lett. **393**, 51 (2004).
[93] O.A. Vydrov, and G.E. Scuseria, J. Chem. Phys. **125**, 34109 (2006).

[94] J.-D. Chai, and M. Head-Gordon, J. Chem. Phys. **128**, 084106 (2008).
[95] J.-D. Chai, and M. Head-Gordon, Phys. Chem. Chem. Phys. **10**, 6615 (2008).
[96] R. Peverati, and D.G. Truhlar, J. Phys. Chem. Lett. **2**, 2810 (2011).
[97] L.A. Curtiss, P.C. Redfern, and K. Raghavachari, J. Chem. Phys. **126**, 084108 (2007).
[98] L.A. Curtiss, P.C. Redfern, and K. Raghavachari, J. Chem. Phys. **127**, 124105 (2007).
[99] B. Chan, J. Deng, and L. Radom, J. Chem. Theory Comput. **7**, 112 (2011).
[100] L.A. Curtiss, K. Raghavachari, P.C. Redfern, V. Rassolov, and J.A. Pople, J. Chem. Phys. **109**, 7764 (1998).
[101] L.A. Curtiss, P.C. Redfern, K. Raghavachari, V. Rassolov, and J.A. Pople, J. Chem. Phys. **110**, 4703 (1999).
[102] A.G. Baboul, L.A. Curtiss, P.C. Redfern, and K. Raghavachari, J. Chem. Phys. **110**, 7650 (1999).
[103] J.A. Montgomery Jr., M.J. Frisch, J.W. Ochterski, and G.A. Petersson, J. Chem. Phys. **110**, 2822 (1999); *ibid*. **112**, 6532 (2000).
[104] J.W. Ochterski, G.A. Petersson, and J.A. Montgomery Jr., J. Chem. Phys. **104**, 2598 (1996).
[105] S. Grimme, J. Chem. Phys. **118**, 9095 (2003).
[106] M. Pitonak, P. Neograd, J. Cerny, S. Grimme, and P. Hobza, Chem. Phys. Chem. **10**, 282 (2009).
[107] S. Grimme, J. Comput. Chem. **24**, 1529 (2003).
[108] T. Takatani, E.E. Hohenstein, and C.D. Sherrill, J. Chem. Phys. **128**, 124111 (2008).
[109] M. Pitonak, J. Rezac, and P. Hobza, Phys. Chem. Chem. Phys. **12**, 9611 (2011).
[110] H.Y. Afeefy, J.F. Liebman, and S.E. Stein, Neutral Thermochemical Data. In *NIST Chemistry WebBook, NIST Standard Reference Database Number 69*, edited by P.J. Linstrom, and W.G. Mallard (National Institute of Standards and Technology, Gaithersburg, MD) http://webbook.nist.gov.
[111] An uncertainty of 3.8 kJ mol^{-1} is assigned to the W1-F12 heats of formation (taken to be twice the RMSD reported in ref. 18 for a set of 97 first-row molecules). This should be regarded as a conservative error bar since the molecules involved in the EIE22 dataset are largely dominated by dynamical correlation effects (see Computational Methods).
[112] P. Mori-Sanchez, A.J. Cohen, and W. Yang, J. Chem. Phys. **125**, 201102 (2006).
[113] A. Halkier, T. Helgaker, P. Jørgensen, W. Klopper, H. Koch, J. Olsen, and A.K. Wilson, Chem. Phys. Lett. **286**, 243 (1998).